Design Optimization of a Capacitive Sensor for Mass Measurement of Nanometer-Sized Exhaust Carbon Particles

Vaishali Sanjay Kulkarni[1,*], Suvarna Sandip Chorage[2]

[1]Department of Electronics and Telecommunication Engineering, All India Shri Shivaji Memorial Society's Institute of Information Technology, Savitribai Phule Pune University, Pune, India

[2]Department of Electronics and Telecommunication Engineering, Bharti Vidyapeeth's College of Engineering for Women, Savitribai Phule Pune University, Pune, India

Abstract

Nanometer-sized carbon particulates generated by incomplete combustion in heavy-duty vehicles are harmful to human health. A high-resolution technique is needed to detect and measure these pollutants. This study aims to optimize a capacitive sensor design for detecting and measuring particulates. Firstly, the effect of design parameters on particulate detection and sensor compliance sensitivity is investigated by using the finite element method. By comparing the simulation results with literature findings for performance validation, the sensor structure is optimized to detect lower particulate concentrations. The simulation result shows that particulate detection sensitivity has linear variations with changes in particulate mass. With optimum electrode spacing and top insulation layer thickness of 5 µm, the sensor can detect a particulate deposition of 0.033 mg/min and generate a maximum capacitance of 581 pF. Since the optimized design can measure particulate deposition at a lower range and with higher sensitivity, it is suitable to be applied to detect nanometer-sized carbon particulates.

1. Introduction

Carbon particulates are a major contributor to environmental pollution and ozone layer damage, ranging in size from 20 to 100 nanometers. These particulates may include soot particles, particulate matter, or carbon black, and pose a severe health risk to individuals. A particulate filter is used in vehicle systems to reduce emissions of this pollutant. Exhaust systems detect carbon particles using pressure sensors which measure pressure differences due to particle accumulation. A pressure difference is, therefore, an indication of particulate filter failure. An alternative manual method of measuring particulate mass uses nanometer-sized filter paper in smoke collection machines to collect particulates. This method estimates particulate mass manually by identifying the presence of particulates on the filter paper.

The existing particulate detection method uses resistance-based sensors that serve only as a detection facility but cannot measure the particulate mass [1]. Resistance-based sensing involves either an accumulative electrode or a charge-based deposition method [2], with large-sized particle tracking being complex. It is, therefore, vital to consider the Lagrangian and Eulerian modeling methods for gas particulate modeling [3]. While Eulerian modeling is less complicated, it is more time-consuming than Lagrangian modeling [4]. The literature mainly uses electromechanical, interdigitated electrode systems for gas sensing due to their minute dimensions, with these electrodes resembling the interlocking fingers of two clapped hands

---

* Corresponding author. E-mail address: vaishsan2000@gmail.com

and having an electric field used to build capacitance [5-6]. Capacitive sensors are ideal for their low static power consumption [7-9] and find use in various fields, such as biomedical, automotive, robotics, and gas sensing. Capacitive sensors can also detect and measure volatile organic compounds [10-12]. Microsensors have been widely used in sensing since the 1960s [13], indicating a need for a systematic study of sensor models, features, and design issues.

Further research needs to also explore the factors that influence sensitivity distribution and the impact of conductivity on the performance of capacitive sensors. The electrode geometry significantly affects the sensor's sensitivity [14]. An electronic nasal pod (ENP) is a wearable device capable of preventing allergies and sensing air pollutants. To fabricate a 3D-printed ENP, a high-efficiency particulate air (HEPA) filter is integrated for sieving pollutants at the first stage. The ENP uses three electrodes to sense oxygen electrochemically using a potentiostat [15]. A novel pressure sensor has also been developed to perform sensing based on changes in the overlapping areas of electrodes rather than their separation. This sensor, which has a square membrane of 2.5 mm × 2.5 mm, can provide a total capacitance change of 0.365 pF for an applied pressure of 0-100 KPa [16].

Insights into the trade-off between sensor design parameters and sensor requirements were revealed in a study that focused on optimizing capacitive sensors [17]. An innovative capacitive moisture sensor was designed for polymers to demonstrate the relationship between the sensor's geometrical parameters and performance [18]. Despite the limitations associated with some commonly used microelectromechanical systems (MEMS) design methods, evolutionary computations have recently become famous for designing and optimizing MEMS [19].

A model based on a MEMS capacitive sensor demonstrated that finite element analysis is the most accurate technique for estimating sensor capacitance [20]. Interdigitated capacitive sensors were used in mining environments to monitor real-time nanoscale particle concentrations, with simulations indicating that the sensor response is proportional to the number of particles accumulated on the sensor [21]. COMSOL, a tool for modeling and simulating SnO_2/rGO gas sensors, was used to detect and characterize NO_2 [22].

A complete mass sensing module was achieved by integrating a TPoS MEMS oscillator, MEMS, circuit, and air flow technologies to develop a PM2.5 sensor [23]. A thin film circular diaphragm was developed for MEMS resonant mass sensors that detect airborne particles, demonstrating real-time detection of standard silica microspheres [24]. To measure PM2.5 and PM10, an air pollution monitoring device with a particle matter sensor was used [25]. A study which investigated low-cost PM sensors proposed methods to correct the error factors caused by the optical scattering method [26]. A piezoelectric resonating membrane operates the gravimetric-based particulate matter sensor for portable applications, and future work includes implementing a thermophoresis mechanism to remove residual particles deposited on the sensor during measurements [27]. While few modeling and simulation reports exist on sensors designed for detecting and measuring carbon particulates, there is ample scope for developing micro-level devices to accomplish this.

This study shows the result of the design optimization of the proposed particulate sensor and evaluates its effectiveness by interpreting the results. The study focuses on predicting particle deposition and the corresponding electric field strength of particulate sensors through computational fluid dynamics (CFD) and electric field simulations. The work is novel because it optimizes sensor design parameters and measures the particulate mass with high precision to a minimum value.

However, there were several challenges, such as determining the period of particulate deposition and integrating the deposited mass with electrical simulations. Much of the effort was devoted to the mathematical modeling of CFD and the execution of electric field simulations. Modeling the nanoparticle sensor in both the electrical and mechanical domains was challenging, especially due to the fragile top insulation layer, which had a thickness of 5 μm. However, this layer is crucial for achieving high sensitivity. The results of the sensor model development, simulation method, simulation cases, and particulate detection are presented in detail.

2. An Optimized Sensor Design Dimensions

Fig. 1 presents the sensor layout with dimensions, cross-section, and materials. The dimensions are optimized through iterations to obtain capacitance with good resolution. The sensor substrate size is mm × 10 mm, while the sensor structure is an interdigitated electrode with an electrode length of 4300 µm, spacing of 5µm, and width of 100 µm. The sensor uses 38 electrodes. Fig.1 (b) shows a cross-section of the optimized sensor with a substrate and top insulation layer of Si_3N_4.

(a) Optimized dimensions (µm)   (b) Cross-section of IDC
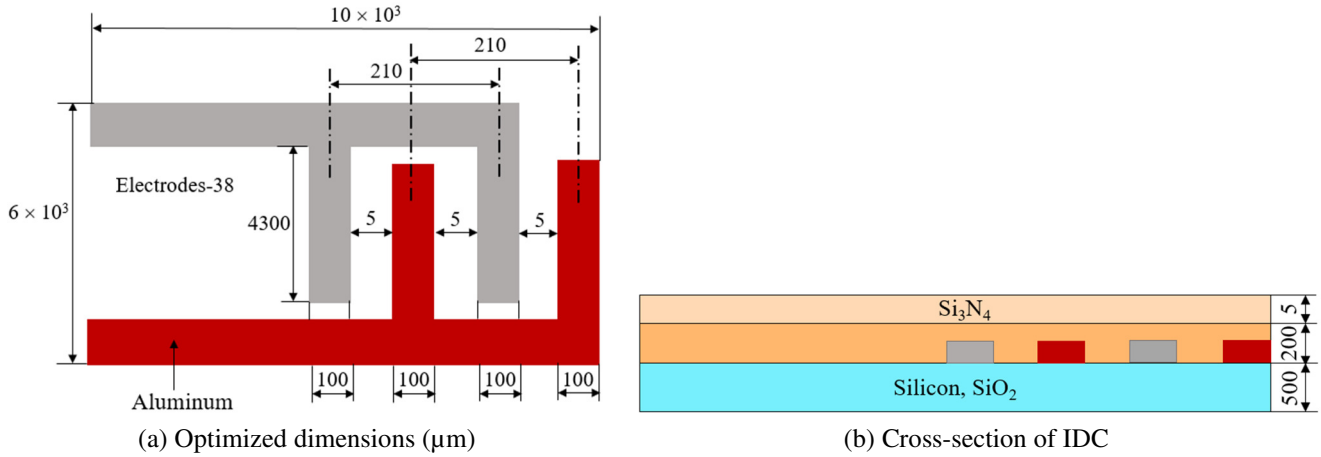
Fig. 1 The layout of interdigitated electrode capacitor (IDC) [2]

2.1. Methodology, material properties, and boundary definitions

Fig. 2 shows a two-dimensional (2D) model of a single-unit cell. Physical materials and boundaries used for simulations are defined as shown in Fig. 3. For the design requirements and a temperature of 473℃, the relative permittivity values are 3.6 for silicon dioxide, 9.5 for silicon nitride, and 1 for air. The analysis considers deposition in accumulative mode with the particulate diameters ranging from 0.01 mm to 100 mm. The simulations use a gas flow velocity of 38 m/s to 47 m/s and a particulate density of 1150 kg/m^3. According to the calculations, the estimated density of the mixture (air plus soot) is 0.48109 kg/m^3. The soot concentrations in terms of volume and mass are 8.0×10^{-06} and 0.019123, respectively.
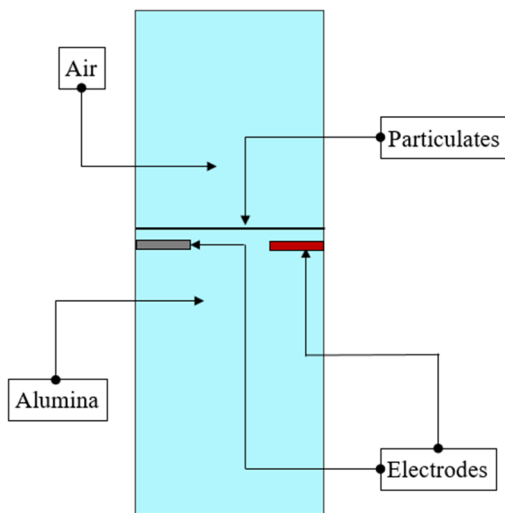

Fig. 2 2D model of one unit cell for analysis and simulation of electrostatic fields
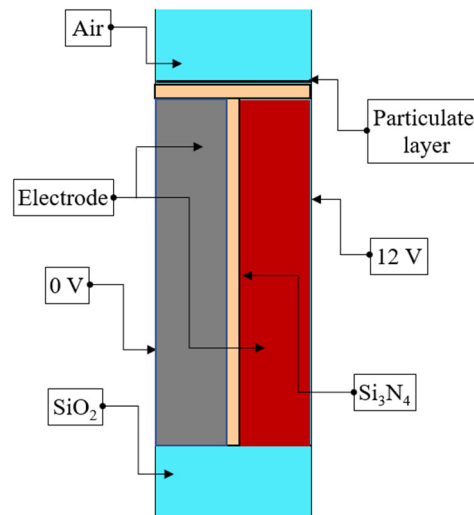
Fig. 3 Model of a sensor unit cell with a particulate layer for analysis with defined boundaries

The static analysis applies a boundary condition of zero charges to all external edges of the sensor. The voltages at sensor terminals 1 and 2 are 0 V and 12 V, respectively. The parametric sweep function in COMSOL allows the particulate layer to gradually increase from 0.1 µm to 2 µm with a step size of 0.1 µm and particulate diameters between 10 µm and 100 µm. As a result, the electric field and capacitance values are subject to variation.

2.2. Design requirements

(1) Optimize the sensor design dimensions to extract the maximum capacitance value.

(2) Obtain high sensitivity to low particulate deposits.

(3) Detect and estimate time intervals of particulate deposition.

(4) Withstand temperatures up to 400°C.

(5) Optimize the design of experiments (DOE) study to predict change in the capacitance for particulate disposition.

3. Equations Governing Physics

The two components of the analysis are the CFD and the electrical. The CFD component analyzes the flow characteristics to predict the mass of particulates at the sensor surface. The electrical component evaluates the sensor's effectiveness to predict its electrical properties. The electrostatics domain and CFD model are closely coupled due to the influence of particulate mass.

$$\rho(u \times \nabla)u = \nabla \left\{ -pl + (\mu + \mu T)\left[Vu + (\nabla u)^T \right] - \frac{2}{3}(\mu + \mu T)(\nabla \times u)l \right\} + F \tag{1}$$

$$\nabla \times pu = 0 \tag{2}$$

$$\rho(u \times \nabla)k = \nabla \left[\left(\mu + \frac{\mu T}{\sigma_\in} \right) \nabla k \right] + Pk - \rho \in \tag{3}$$

$$\rho(u \times \nabla)k = \nabla \left[\left(\mu + \frac{\mu T}{\sigma_\in} \right) \nabla \in \right] + C_{\in 1} \frac{\in}{k} Pk - C_{\in 2} \rho \frac{\in^2}{k} \tag{4}$$

$$\in = e \times p \tag{5}$$

$$\mu_T = \rho \times C_u \frac{k^2}{\in} \tag{6}$$

$$Pk = \mu_T \left[\Delta u : \Delta u + (\Delta u)^T - \frac{2}{3}(\Delta \times u)^2 \right] - \frac{2}{3} \rho k \Delta \times u \tag{7}$$

ρ = Density (kg/m³), T = Absolute temperature (K), p = Pressure (Pa), u = Velocity vector (m/s), μ = Dynamic viscosity (Pa.s), F = Volume force vector (N/m³), V = Velocity (m/s), ep = Turbulent dissipation rate, q = Heat flux by conduction (W/m²), k = Thermal conductivity (W/m.K) (heat transfer), k = Turbulent kinetic energy (Turbulent flow), Cp = Specific heat (J/kg.K).

The equations presented in this section describe the physics underlying the computational models. The equations solved are the Reynolds-averaged Navier-Stokes (RANS) equations for the conservation of momentum and the continuity equation for the conservation of mass [23].

The solver calculated that a single particulate would take 5.7 ms to reach the sensor. Therefore, the transient solver's period is set to 0-15 ms, with a time step of 0.5 ms. The modeling uses an electrostatic (es) interface to calculate the electric field, displacement field, and distribution of the dielectric potential. For in-plane 2D modeling, the electrostatic interface assumes symmetry, and the electric field, E, is tangential to the XY plane.

$$E = -\nabla V \tag{8}$$

The electric field, V, is defined by Eq. (8) in static conditions. Adding Eq. (8) to the constitutive relationship $D = \varepsilon_0 E + P$.

$$-\nabla \times \left(\varepsilon_0 \nabla V - P \right) = \rho \qquad (9)$$

The modeling presents Gauss' law as a relationship between the electric displacement, D, and the electric field, E, given by Eq. (9). The permittivity of vacuum is ε_0 with SI units of F/m, the vector of electric field polarization is P, with SI units of C/m^2, and the density of space charges is ρ, with SI units of C/m^3. The equation describes the electrostatic field of a dielectric material. For in-plane 2D modeling, the electrostatic interface assumes symmetry, and the electric field, E, is tangential to the XY plane.

$$-\nabla \times d \left(\varepsilon_0 \nabla V - P \right) = \rho \qquad (10)$$

The thickness of the Z-direction given by d and the physics interface solves this Eq. (10).
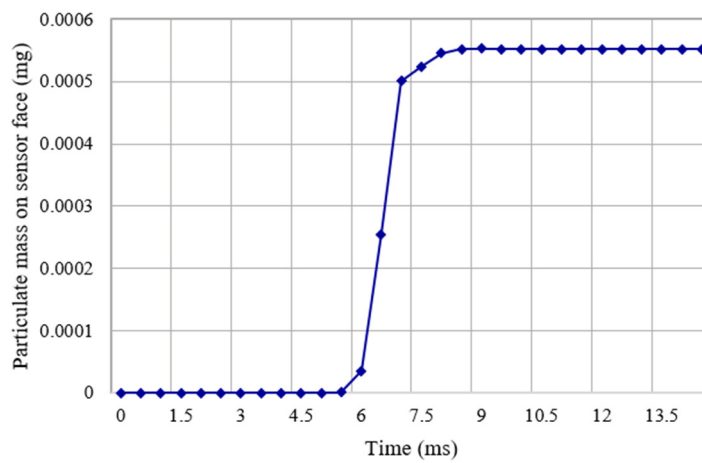
4. Particulate Mass Estimation

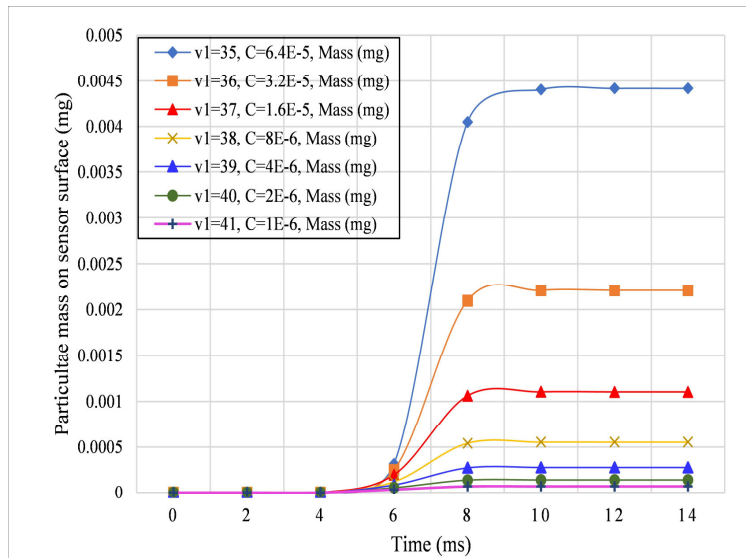Fig. 4 The deposited mass on the sensor face (0 to 15 ms)

Fig. 5 Results of DOE - S-Curve behavior

A steady-state analysis is performed on the sensor model to determine its electric potential field and capacitance. An electrostatic node is added to the model to solve electrical field and capacitance physics. Fig. 4 shows a plot of the particulate mass and derived mass values from 0 to 15 ms. The highest gas velocity reaches 48.5 m/s between 0 and 15 ms, propagating from the sensor surface. The fluid pressure gradually increases to 1.02×10^{-05} at 6.5 ms and remains constant until 15 ms. The correlation between the deposited mass and sensor capacitance results in a total deposition of 0.033 mg over 60 seconds. A

maximum mass of 24.8 mg/s can be calculated based on the mass volume fraction of the 8.0×10^{-06} sensor location, with gases flowing at 24.8 mg/s to the sensor surface and exiting at the outlet into the atmosphere. The finite element analysis reveals a particulate deposition rate of 0.0005 g/s on the sensor surface between 0 and 15 ms, which remains constant for one second. Thus, it is possible to estimate the deposition rate over an extended period. The analysis also proves that the deposited mass on the sensor face (0 to 15 ms) is proportional to the gas flow.

Fig. 5 shows that particulate mass accumulation is crucial to the outcome. Designed experiments to broaden the scope of work for flow rate/velocity and particulate concentration. The flow velocity, v1, ranges from 35 m/s to 41 m/s, and the particulate concentration from 6.4×10^{-05} to 1.0×10^{-06}. A DOE study indicates that the total mass deposited ranges from 0.000069 mg at v1 = 41 m/s and C = 1×10^{-06} to 0.0044 mg at v1 = 35 m/s and C = 6.4×10^{-05} during the 15 ms period. As noted in the sensor's response time and sensitivity, the sensor shows a fast response time of 4.8 milliseconds to low-mass depositions.

5. Modeling of Incremental Particulate Layer Capacitance

The incremental particulate layer sensor models the electric potential distribution and the resulting capacitance. Fig. 6 presents the capacitance values as extracted from COMSOL contour plots. The magnitudes of electric potential at various layer thicknesses (0.1 µm to 2 µm in 0.5 µm steps) in the sensor domain are extracted and plotted in Fig. 7. As the results show, the capacitance of the sensor increases from 566 pF to 568 pF, revealing a linear relationship between the detection time and the deposited particulates on the sensor surface.
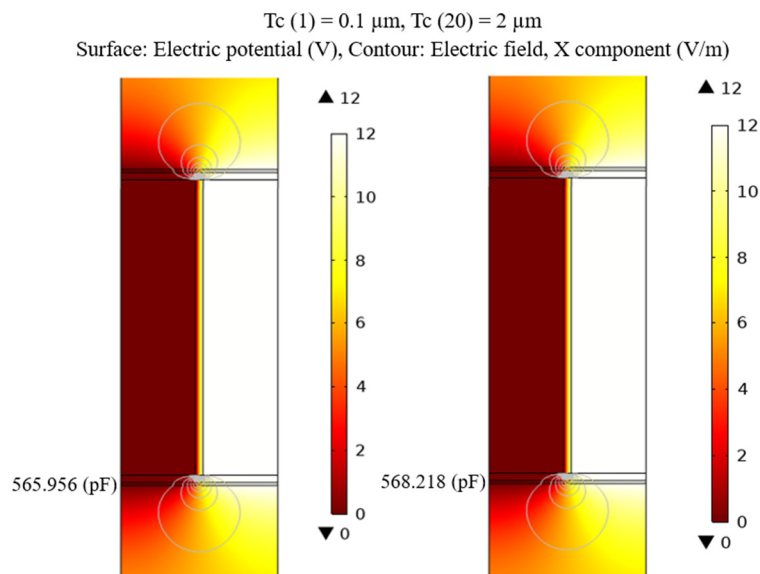

Fig. 6 Electrical potential (V) versus (Tc-soot layer thickness) at 0.1 µm and 2 µm

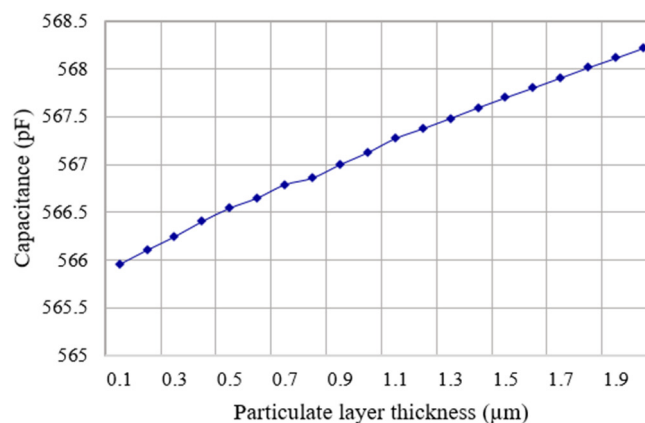Fig. 7 Sensor capacitance (soot layer thickness Tc = 0.1 µm to 2 µm)

An electrical capacitance in pF is measured through electrical simulations to determine the particulate deposition in mg. The sensor showed a linear response within the low particulate deposition ranges. Fig. 8 illustrates micro capacitance extracted for the corresponding thicknesses of the deposited particulate layer. Accordingly, in Fig. 9, the masses are plotted on the X-axis against the corresponding extracted capacitance on the Y-axis, with the maximum capacitance of 581 pF corresponding to a mass of 0.05 mg.
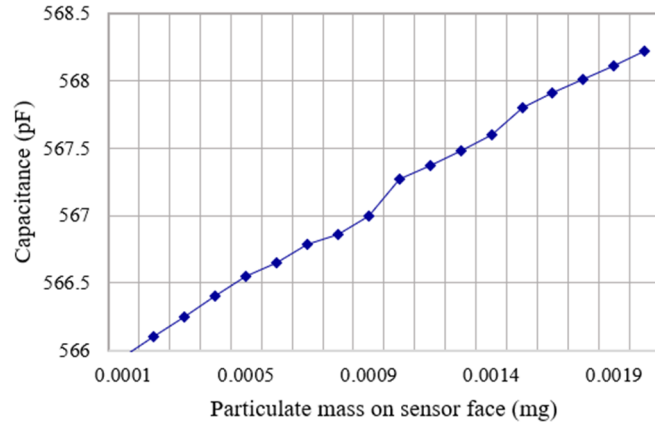
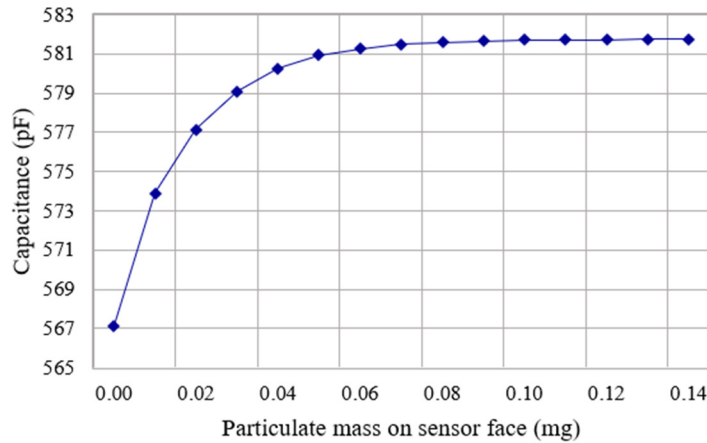Fig. 8 Sensor capacitance for mass-deposited (mg)

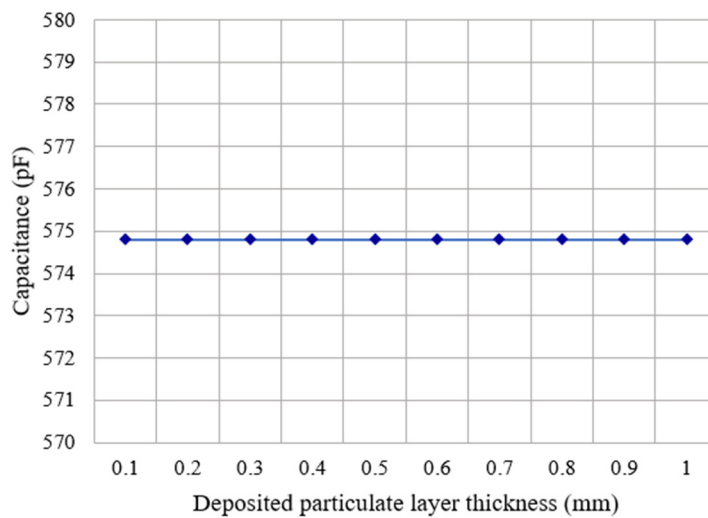Fig. 9 The mass plot (Tc = 1 to 1000 µm) after 0.05 mg

Fig. 10 The effect of increasing the thickness of the top insulation layer

The analysis and simulation results indicate that the sensor operates linearly as the particulate layer thickness increases from 0.1 µm to 2 µm. Fig. 8 illustrates the corresponding increase in capacitance. There is a micro-level increment in capacitance as the thickness of the deposited mass increases, the formation of agglomerates being responsible for this micro-

level increment. Also, the mass plot (Tc = 1 to 1000 µm) exhibits saturated behavior after 0.05 mg, as shown in Fig. 8. By using capacitance values derived from CFD simulations, the incremental layer thickness values are converted to particulate masses, measured in mg.

Modeling incremental particulate layer capacitance with an increased thickness of the top insulation layer. The sensor's dimensions are optimized to reflect linear capacitance variations with a top insulation thickness of 5 µm. The sensor capacitance measurement has a mass detection limit of 0.05 mg. Results show that the thickness of the insulation layer on the top of electrodes directly affects the sensor's sensitivity. Fig. 10 illustrates the effect of increasing the thickness of the insulation layer to 0.5 mm. As the thickness of the top insulation layer increases, the sensor's sensitivity decreases, resulting in a constant capacitance and no significant change in the sensor's output capacitance.

6. Comparison of Sensor Performance with Literature-Based Benchmarks

Hagen et al. [2] highlighted the experimental dimensions and developed a 2D CAD model of the sensor with electrodes using COMSOL. The dimensions of the device measure equal electrode width and spacing of 100 µm, an electrode thickness of 4 µm, and an electrode length of 48 µm. The reference device has a substrate thickness of 635 meters and an insulation layer of 8 meters, with 29 electrodes.

The predicted capacitance values in the reference sensor agree with the experimental data, with an error margin of ±5%. However, the measured capacitance values (ranging from a minimum of 8.40 pF to a maximum of 50.49 pF) are too small to be used for mass measurement. As a result, it is necessary to estimate the maximum electrostatic field by optimizing the design dimensions.

A subsequent study provided insights that enabled the optimization of the sensor's design. This optimization enhanced the sensor's selectivity and sensitivity for detecting and measuring particulates, as presented in this paper. A 2D model of the sensor was developed in COMSOL, which reduced both computational time and costs. The software module developed for the sensor analysis can serve as a proven design tool for screening various IDC layouts. Furthermore, this simulation module could be applied to estimate the expected sensor's sensitivity.

Hagen et al. [2] also discussed how the findings of an experiment with a sensor that could not measure mass contributed to the development of an improved sensor. The optimized sensor proves its superiority to the experimental one in [2], as it can measure particulate deposition at a lower range and with higher sensitivity.

7. Conclusions

This study presented an electrostatic simulation of an optimized capacitive sensor design that can detect nanometer-sized carbon particulates at the lowest possible level. CFD simulations were conducted to model the deposition of particulate mass on the sensor surface. The amount of particulate mass based on time and mixture flow was predicted, and the contour plots of electric potential distribution and sensor capacitance values for the optimized capacitive sensor design were illustrated. The predicted sensor capacitance increases with the rising of the particulate deposition. The study also compared the optimized sensor with the benchmark design [2] and illustrated the performance improvements achieved with the optimized design.

Given the forthcoming emission norms worldwide, it is imperative to address mass estimation promptly. A threshold-based corrective action approach based on the results can significantly reduce environmental emissions. It would be helpful to assess the performance of the sensor before prototyping begins. The results indicate that particulate detection sensitivity increases with decreasing insulating layer thickness, and the optimized sensor produces ten times more output than the benchmark sensor. In addition, the presented sensor design incorporates interdigitated electrodes, making it convenient, durable, and reliable to operate at room temperature.

However, due to high levels of deposition, the sensor becomes saturated, requiring regeneration and calibration to accommodate dynamic conditions. Accordingly, future work should focus on optimizing sensor location, designing sensor mounts that minimize back pressure, and optimizing electromagnetic parameters for optimum sensing performance.

Conflicts of Interest

The authors declare no conflict of interest.

References

[1] H. Husted, G. Roth, S. Nelson, L. Hocken, G. Fulks, and D. Racine, "Sensing of Particulate Matter for On-Board Diagnosis of Particulate Filters," SAE International Journal of Engines, vol. 5, no. 2, pp. 235-247, May 2012.

[2] G. Hagen, M. Feulner, R. Werner, M. Schubert, A. Muller, G. Riess, et al., "Capacitive Soot Sensor for Diesel Exhausts," Sensors and Actuators B: Chemical, vol. 236, pp. 1020-1027, November 2016.

[3] B. Zhao, C. Chen, X. Yang, and A. C. K. Lai, "Comparison of Three Approaches to Model Particle Penetration Coefficient through a Single Straight Crack in a Building Envelope," Aerosol Science and Technology, vol. 44, no. 6, pp. 405-416, April 2010.

[4] P. Sydenham and R. Thorn, Handbook of Measuring System Design, vol. 2, UK: John Wiley & Sons, 2005.

[5] A. V. Mamishev, K. Sundara-Rajan, F. Yang, Y. Du, and M. Zahn, "Interdigital Sensors and Transducers," Proceedings of the IEEE, vol. 92, no. 5, pp. 808-845, May 2004.

[6] C. Sapsanis, H. Omran, V. Chernikova, O. Shekhah, Y. Belmabkhout, U. Buttner, et al., "Insights on Capacitive Interdigitated Electrodes Coated with MOF Thin Films: Humidity and VOCs Sensing as a Case Study," Sensors, vol. 15, no. 8, pp. 18153-18166, August 2015.

[7] C. Sapsanis, S. Sivashankar, H. Omran, U. Buttner, and K. N. Salama, "Capacitive Immunosensor for C-Reactive Protein Quantification," IEEE 58th International Midwest Symposium on Circuits and Systems (MWSCAS), August 2015.

[8] H. Omran, M. Arsalan, and K. N. Salama, "A Robust Parasitic-Insensitive Successive Approximation Capacitance-to-Digital Converter," Proceedings of the IEEE 2014 Custom Integrated Circuits Conference, September 2014.

[9] H. Omran, M. Arsalan, and K. N. Salama, "7.9 pJ/Step Energy-Efficient Multi-Slope 13-bit Capacitance-to-Digital Converter," IEEE Transactions on Circuits and Systems II: Express Briefs, vol. 61, no. 8, pp. 589-593, August 2014.

[10] J. W. Gardner, P. K. Guha, F. Udrea, and J. A. Covington, "CMOS Interfacing for Integrated Gas Sensors: A Review," IEEE Sensors Journal, vol. 10, no. 12, pp. 1833-1848, December 2010.

[11] P. W. Oluwasanya, G. Rughoobur, and L. G. Occhipinti, "Design, Modeling and Simulation of a Capacitive Size-Discriminating Particulate Matter Sensor for Personal Air Quality Monitoring," IEEE Sensors Journal, vol. 20, no. 4, pp. 1971-1979, February 2020.

[12] R. S. Jachowicz and S. D. Senturia, "A Thin-Film Capacitance Humidity Sensor," Sensors and Actuators, vol. 2, pp. 171-186, 1981-1982.

[13] X. B. Li, S. D. Larson, A. S. Zyuzin, and A. V. Mamishev, "Design Principles for Multichannel Fringing Electric Field Sensors," IEEE Sensors Journal, vol. 6, no. 2, pp. 434-440, April 2006.

[14] X. Hu and W. Yang, "Planar Capacitive Sensors – Designs and Applications," Sensor Review, vol. 30, no. 1, pp. 24-39, 2010.

[15] A. Kothuru and S. Goel, "Electronic Nasal Pod: A 3D Printed Device to Filter and Electrochemically Detect Pollutants," IEEE Sensors, October 2020.

[16] S. Zargari, S. Falaki, and H. Veladi, "Design and Finite Element Analysis of a MEMS Based Capacitive Pressure Sensor Using CNT/PDMS Nanocomposite Electrodes," 24th Iranian Conference on Electrical Engineering, May 2016.

[17] Y. Huang, Z. Zhan, and N. Bowler, "Optimization of the Coplanar Interdigital Capacitive Sensor," AIP Conference Proceedings, vol. 1806, no. 1, article no. 110017, February 2017.

[18] R. M. D. Santos, J. M. Sallese, M. Mattavelli, A. S. Nunes, C. Dehollain, and D. Barrettino, "High Precision Capacitive Moisture Sensor for Polymers: Modeling and Experiments," IEEE Sensors Journal, vol. 20, no. 6, pp. 3032-3039, March 2020.

[19] P. Wang, Q. Lu, and Z. Fan, "Evolutionary Design Optimization of MEMS: A Review of Its History and State-of-the-Art," Cluster Computing, vol. 22, no. 4, pp. 9105-9111, July 2019.

[20] P. W. Oluwasanya, G. Rughoobur, and L. G. Occhipinti, "Comparison of Analytical and Numerical Methods of Obtaining Coplanar Capacitance of Microelectrodes for Particulate Matter Detection," IEEE Sensors Journal, vol. 20, no. 15, pp. 8631-8636, August 2020.

[21] D. Back, D. Theisen, W. Seo, C. S. J. Tsai, and D. B. Janes, "Development of Interdigitated Capacitive Sensor for Real-Time Monitoring of Sub-Micron and Nanoscale Particulate Matters in Personal Sampling Device for Mining Environment," IEEE Sensors Journal, vol. 20, no. 19, pp. 11158-11597, October 2020.

[22] F. Y. Niyat and M. H. S. Abadi, "COMSOL-Based Modeling and Simulation of SnO2/rGO Gas Sensor for Detection of NO2," Scientific Reports, vol. 8, article no. 2149, February 2018.

[23] C. H. Weng, G. Pillai, and S. S. Li, "A PM2.5 Sensor Module Based on a TPoS MEMS Oscillator and an Aerosol Impactor," IEEE Sensors Journal, vol. 20, no. 24, pp. 14722-14731, December 2020.

[24] F. Foncellino, L. Barretta, E. Massera, and A. Corigliano, "Piezoelectric MEMS for Microparticles Detection," IEEE Sensors, October-November 2021.

[25] P. Das, S. Ghosh, S. Chatterjee, and S. De, "A Low Cost Outdoor Air Pollution Monitoring Device with Power Controlled Built-In PM Sensor," IEEE Sensors Journal, vol. 22, no. 13, pp. 13682-13695, July 2022.

[26] H. Cho and Y. Baek, "Practical Particulate Matter Sensing and Accurate Calibration System Using Low-Cost Commercial Sensors," Sensors, vol. 21, no. 18, article no. 6162, September 2021.

[27] N. Singh, M. Y. Elsayed, and M. N. El-Gamal, "Towards the World's Smallest Gravimetric Particulate Matter Sensor: A Miniaturized Virtual Impactor with a Folded Design," Sensors, vol. 22, no. 5, article no. 1727, March 2022.